

## Effects of Microstructure on Fiber-Matrix Debonding of Metal Matrix Composites under Transverse Loading

Mohammad Tahaye Abadi  
Aerospace Research Institute  
Tehran, Iran  
E-mail: abadi@ari.ac.ir

**Abstract**—A micromechanics damage model is presented to examine the effect of microstructures on the fiber–matrix debonding for unidirectional carbon fiber reinforced metal matrix composites under the transverse loading. Microstructure is represented by a repeating unit cell (RUC). Two fiber arrays are considered including ideal square fiber packing and random fiber packing defined by random sequential algorithm. A cohesive zone model is used to predict the onset of fiber–matrix debonding while the non-linear behavior in the matrix phase is modeled using the von-Mises plasticity theory. The micromechanical results show that the damage evolution starts at a lower stress level in the microstructure with random fiber packing compared to the regular microstructure and the transverse stress converges to the same level in both microstructures at high strain value. Micromechanical modeling procedure provides detail viewpoint into the microscopic damage accumulation prior to ultimate failure and highlights the different roles of the fiber–matrix debonding and matrix plasticity in the macroscopic response of the composite.

**Keywords**—*debonding; micromechanical modeling; transverse loading*

### I. INTRODUCTION

Metal matrix composites have found many applications as constructional and functional materials in different industries. The presence of reinforcement in metal matrix materials improves the properties such as the tensile strength, creep resistance, fatigue strength, thermal shock resistance, and corrosion resistance. Transverse strength of composite materials is one of the limiting design criteria in composite structures. Fiber-matrix interfaces are subjected to high local stress levels and have a greater propensity to undergo damage nucleation than those in dilute regions [1]. Transverse fracture is a result of fiber–matrix debonding and/or matrix micro-cracking which can induce further damages in laminates such as inter-ply delamination or fiber fracture in adjacent plies through the process of damage accumulation [2, 3]. Due to the complex nature of damage progression, many micromechanical studies have focused on transverse fracture behavior from viewpoint of damage initiation and evolution [4-7].

The micromechanics techniques yield information on both macroscopic and microscopic levels which are used for the prediction of the overall characteristics in view of continuum mechanics as well as the evaluation of the

potential failure modes leading to the ultimate failure of heterogeneous materials [8, 9]. The micromechanical model provides an efficient procedure to determine and design the properties of composite materials.

Fiber-matrix interfaces have been modeled in a number of ways including a narrow region of continuum with graded properties, an infinitely thin surface separated by springs, and cohesive zones with specific traction–separation relations [6]. In the spring layer model [7], a stress based criterion for debonding and a frictional resistance based criterion for interfacial sliding have been used to capture debonding and sliding. Debonding is postulated to occur under the combined loading conditions at the interface. The cohesive zone approach is being increasingly used in describing fracture and failure behavior in a number of material systems [4, 5].

The transverse fracture behavior of composite materials depends on numerous contributing factors, such as constituent properties, interfacial strength, process related defects, and local morphological parameters like volume fraction, size, shape and spatial distribution of reinforcements. The present research works determines the influence of microstructure on the elastic-plastic properties of metal matrix composites considering the debonding at the fiber-matrix interface at high transverse loading. A micromechanical modeling procedure is implemented to evaluate the response of unidirectional continuous fiber composites subjected to finite axial deformation. The microstructure of the metal matrix materials is represented by a repeating unit cell (RUC) considering two fiber arrangements including ideal square fiber packing and random fiber packing defined by random sequential algorithm. The Volume averaging scheme is implemented to apply the local macroscopic deformation gradient tensor to the RUC assigned to the microstructure. The micromechanical modeling procedure is implemented for graphite/aluminum metal matrix composite in which the reinforcement behaves as elastic, isotropic solids and the matrix was modeled as an isotropic elastic-plastic solid following the von Mises criterion with isotropic hardening [10] and the Ramberg-Osgood relationship [11] is assumed between equivalent true stress and logarithmic strain. A cohesive zone model is used to predict the onset of fiber–matrix debonding, in which the damage initiation is defined based on the normal and shear strength at the interfacial zone. The damage evolution is model considering a exponential softening curve for the

degradation rate of the cohesive stiffness. The RUC is subjected to uniaxial deformation increased to a considerable value to evaluate both elastic and plastic behaviors of metal matrix composites. The yields strength and true elastic-plastic stress are determined for graphite/aluminum composites.

## II. MICROSTRUCTURE CONFIGURATION

The microstructures of unidirectional fiber reinforced composites are commonly described by three fiber arrangement including square, hexahedral and random fiber-packing patterns. The micromechanical results for linear anisotropic elastic materials revealed that the calculated elastic stiffness values for axial and shear deformation are dependent on the fiber packing [12]. Since the microstructures with square and hexahedral fiber-packing patterns are idealized geometrical representations for fiber arrangement, the microstructure with random fiber packing yields more accurate results. At large plastic deformation of anisotropic materials, the results highly depends on the fiber packing and for some fiber arrangement, the deformation locking may be observed at lower strain.

Since the heterogeneities are orders of magnitude smaller than the total body, the deformation field in the vicinity of one inclusion is approximately the same as the deformation field near neighboring inclusions [13]. Experimental observations [5-7] have shown that deformation field in the vicinity of a subvolume is approximately the same as deformation field of the near neighboring subvolumes. The size of subvolume is small enough compared to the total microstructure size so that the effective properties computed from the subvolume are independent of its size and position within the microstructure. Therefore, the microstructure is represented by a periodic unit cell that deforms in a repetitive way. The periodic modeling can be quite useful, because it provides rigorous estimations with a priori prescribed accuracy for various material properties. Microstructure shown in Fig. 1 is considered for the unidirectional continuous fiber composites. The circular fibers with identical radius are dispersed in the microstructure in a random and isotropic manner. It is assumed that the composite material has a periodic microstructure which can be obtained by translating RUC along three orthogonal axes. The fiber distribution in the unit cell is generated using the random sequential adsorption algorithm [14] which ensures a random, isotropic and homogeneous distribution for the fibers within the RUC. The random coordinates in the cross-section of microstructure are generated for the center of circular fibers with specific diameter, denoted by  $d$ . When a fiber intersects the boundaries of unit cell, another fiber is generated on the neighboring unit cell in order to obtain periodic unit cell. The new fiber is added to the microstructure when the distance between the center of a given fiber and the closest fibers previously generated is greater than a minimum values ( $1.1d$ ). Such condition prevents overlapping fibers as well as ensuring adequate

mesh geometry for the matrix material located between fibers. To prevent element distortion during mesh generation, the fiber surface should not be too close (greater than  $0.1d$ ) to the boundary surfaces of the RUC. When such conditions are satisfied, the fiber is added to the unit cell at the generated random coordinates. The procedure is repeated until the fiber volume fraction reaches close to a pre-defined value. The square cross section is considered for unit cell ( $b_2 = b_3$ ) and the ratio of fiber diameter to unit cell dimension ( $d / 2b_2$ ) is set to 0.05.

## III. MICROMECHANICAL MODEL

Micromechanical model provides efficient tool to characterize composite materials from known properties of their constituents and the distribution of the reinforcement in the microstructure through the analysis of a RUC. The essence in micromechanical approach is to replace the heterogeneous structure of the composite by a homogeneous medium with anisotropic properties.

A Lagrangian viewpoint is used to describe the material motion and the components of vectors and tensors are described in a fixed rectangular coordinate system. In the reference configuration of RUC, the position of a typical material particle is expressed with vector  $\mathbf{X}$  (components  $X_i$ ). In the deformed configuration at instance  $t$ , the particle moves to a position described with vector  $\mathbf{x}_{(\mathbf{x},t)}$  (components  $x_i$ ) corresponding to the displacement vector  $\mathbf{u}_{(\mathbf{x},t)}$  (components  $u_i$ ). The deformation is typically described using the deformation gradient tensor, designated by  $\mathbf{F}$ , whose components are given by

$$F_{ij} = \frac{\partial x_i}{\partial X_j} \quad (1)$$

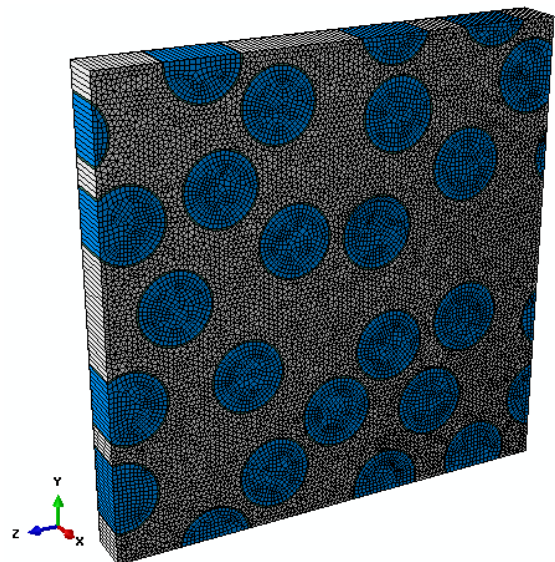


Figure 1. Microstructure of metal matrix composite with random fiber packing.

The reference geometry of RUC is assumed to be a rectangular prismatic volume whose surfaces are parallel to the surfaces defined in a fixed Cartesian coordinate system with origin located at the centre of RUC. The initial dimension of RUC is  $2b_1 \times 2b_2 \times 2b_3$ . The boundary surfaces of reference geometry perpendicular to  $i$ -axis are designated with  $S_i^+$  and  $S_i^-$  intersecting  $i$ -axis at  $X_i = +b_i$  and  $X_i = -b_i$ , respectively. The displacement of the points located on each boundary surface is measured respect to corner points labeled as points  $P_0$ ,  $P_1$ ,  $P_2$  and  $P_3$ . Such points are called reference points. The current position of points located on surface  $S_i^-$  is measured respect to point  $P_0$ , while the position of points located on  $S_1^+$ ,  $S_2^+$  and  $S_3^+$  is measured respect to points  $P_1$ ,  $P_2$  and  $P_3$ , respectively. To enforce the periodicity constraint, the current position of boundary surface is described by [9]:

$$x_{i(-b_1, X_2, X_3, t)} - x_{i(t)}^{(0)} = x_{i(b_1, X_2, X_3, t)} - x_{i(t)}^{(1)} \quad i = \{1, 2, 3\} \quad (2a)$$

$$x_{i(X_1, -b_2, X_3, t)} - x_{i(t)}^{(0)} = x_{i(X_1, b_2, X_3, t)} - x_{i(t)}^{(2)} \quad i = \{1, 2, 3\} \quad (2b)$$

$$x_{i(X_1, X_2, -b_3, t)} - x_{i(t)}^{(0)} = x_{i(X_1, X_2, b_3, t)} - x_{i(t)}^{(3)} \quad i = \{1, 2, 3\} \quad (2c)$$

where  $x_{i(t)}^{(j)}$  are the components of current position vector of corner point  $P_j$ .

To relate the macrostructure deformation to the microstructure deformation, it is assumed that the local macroscopic deformation gradient tensor at a given point to be equal the volume average deformation gradient tensor of RUC assigned at that point. Using the periodicity constraining equations (1), it can be shown [9] that the macroscopic deformation gradient tensor is a function of current position of corner points  $P_0$ ,  $P_1$ ,  $P_2$  and  $P_3$  as follows:

$$F_{ij} = \frac{x_i^{(j)} - x_i^{(0)}}{2b_j} = \frac{u_i^{(j)} - u_i^{(0)}}{2b_j} + \delta_{ij} \quad (3)$$

It should be noted that no summation is considered on  $j$  superscript in Eq. (3).

An energy balance is considered to relate stress tensor in the macroscopic and microscopic scales. The internal power at macroscopic level at a given point is set equal to the internal power in RUC assigned at the corresponding point in a given deformed configuration. It was shown [9] that the energy balance results in

$$\sum_{j=1}^3 \sum_{i=1}^3 \dot{F}_{ji} P_{ij} = \sum_{j=1}^3 \sum_{i=1}^3 \frac{1}{S_i^+} \dot{F}_{ji} \int_{s_i^+} t_j ds \quad (4)$$

where the dot superscript denotes to the time derivative,  $P_{ij}$  are the components of nominal stress tensor defined in macroscopic levels,  $t_j$  are the components of traction force and  $s_i^+$  is the deformed geometry of boundary surface  $S_i^+$ .

#### IV. MATERIAL BEHAVIOR

Aluminum alloy reinforced with stiff graphite fibers is considered. The fibers behaved as elastic, isotropic solids characterized by the elastic modulus  $E_f = 250$  GPa and the Poisson's ratio  $\nu_f = 0.2$ . The matrix is modeled as an isotropic elastic-plastic solid following the von Mises criterion with isotropic hardening [10]. The matrix elastic constants are  $E_m = 70$  GPa and  $\nu_m = 0.33$ , and the Ramberg-Osgood relationship [11] is assumed between equivalent true stress,  $\sigma_m^{eq}$ , and logarithmic strain,  $\varepsilon_m$ , i.e.,

$$\varepsilon_m = \left( \frac{\sigma_m^{eq}}{K} \right)^{1/n} \quad (5)$$

where  $K = 400$  MPa is the strength coefficient and  $n = 0.1$  is the matrix strain hardening exponent [14]. Regarding these data, an initial yield stress of 225.3 MPa is obtained. The aluminum material is reinforced with 0.4 fiber volume fraction.

The damage initiation is defined based on the normal and shear strengths of the cohesive zone in the fiber-matrix interface. Damage is assumed to initiate when the maximum nominal stress ratio reach to a unit value, namely,

$$\max \left( \frac{\langle t_n \rangle}{t_n^0} + \frac{t_s}{t_s^0} + \frac{t_t}{t_t^0} \right) = 1 \quad (6)$$

where symbol  $\langle \rangle$  is Macaulay brackets [15] to signify that a pure compressive deformation or stress state does not initiate damage,  $t_n^0$  and  $t_s^0$  are the normal and shear strengths of the fiber-matrix interfacial zone, respectively. The damage evolution law describes the degradation rate of the cohesive stiffness when the criterion of damage initiation is reached. A scalar damage variable,  $D$ , is introduced to characterize the stiffness degradation as follows:

$$t_n = \begin{cases} (1-D)K_n \delta_n & \delta_n \geq 0 \\ K_n \delta_n & \delta_n < 0 \end{cases} \quad (7a)$$

$$t_s = (1-D)K_s \delta_s \quad (7b)$$

$$t_t = (1-D)K_t \delta_t \quad (7c)$$

The initial value of scalar damage variable is zero before the damage initiation and it is continuously increased up to a unit value as the debonding occurs in the fiber-matrix interface. The damage evolution is modeled based on the level of applied traction or displacement. To describe the evolution of damage under a combination of

normal and shear deformation across the interface, it is useful to introduce an effective displacement defined as [15]

$$\delta_{eq} = \sqrt{\langle \delta_n \rangle^2 + \delta_s^2 + \delta_t^2} \quad (8)$$

A exponential softening curve is considered to model damage evolution at the interface once the maximum stress ratio becomes greater than unit value. The element stiffness reduces until complete failure when the effective displacement reaches to a specific value ( $\delta^f$ ), as shown in Fig. 2. The area under the traction separation determines the fracture energy of cohesive material.

## V. RESULTS

Based on the fiber volume fraction of 0.4, the radius of fiber for microstructure with square fiber packing is  $0.714b_2$ . The fiber-matrix interaction is assumed to be a ring with negligible thickness set to  $0.01b_2$  and the internal surface of ring is tied to the external surface of fiber. The behavior of the fiber-matrix interface is modeled using cohesive elements introducing a displacement discontinuity at the interface when the local stress reaches to the debonding critical condition. A traction-separation law is considered for the fiber-matrix interface to relate the displacement between the top and bottom faces of the cohesive element to the applied normal and shear traction vectors. An initial elastic stiffness was used to ensure the displacement continuity at the interface in the absence of damage. Based on the elastic stiffness values for axial and shear deformation of matrix material and the initial thickness of fiber-matrix interface, the axial and shear stiffness values are set to  $70.0 \times 10^{14}$  Pa/m and  $26.3 \times 10^{14}$  Pa/m, respectively.

### A. Transverse Loading without Damage Evolution

To validate the number of cohesive elements and the corresponding properties of the fiber-matrix interface, the elastic-plastic response is examined before damage initiation for the microstructure with cohesive elements having a perfect bonding between the fiber and matrix materials. The material behavior should be the same in both microstructures before damage evolution. The RUC is subjected to axial transverse strain up to 5% to observe the elastic-plastic behavior of metal matrix composites. The micromechanical modeling procedure is used to apply axial transverse strain to the RUC of the microstructures with random and ideal square fiber packing patterns. The perfect bonding between the fiber and matrix causes considerable distortion in matrix elements at the vicinity of fibers. The presence of cohesive elements considered in the fiber-matrix interface permits radial or tangential separations between fiber and matrix material as the traction vectors exceed a specific critical value. Since no damage evolution criterion is considered in the cohesive elements, the cohesive elements are deformed without decreasing stiffness. When lower axial and shear stiffness values are selected for cohesive elements, negligible strain

is observed in the matrix and fiber materials and the deformation is limited to the cohesive elements and low stress value is determined for composite material. More axial and shear stiffness values considerably reduce the deformation of cohesive elements and simulate perfect bonding at the fiber-matrix interface. The higher stiffness of cohesive elements causes that the numerical procedure tends to diverge when the damage evolution is considered. Fig. 3 illustrates the Cauchy stress-strain curves obtained for RUC with cohesive elements in the microstructures with square and random fiber packing patterns. Since negligible difference is observed between graphs obtained for each microstructure, the presence of cohesive elements predicts the response of perfect microstructure. Both microstructures predict the same yield strength for composite materials. Since the fibers can move between each other in axial deformation of the microstructure with random fiber packing, lower stress requires applying plastic strain compared to microstructure with square fiber-packing.

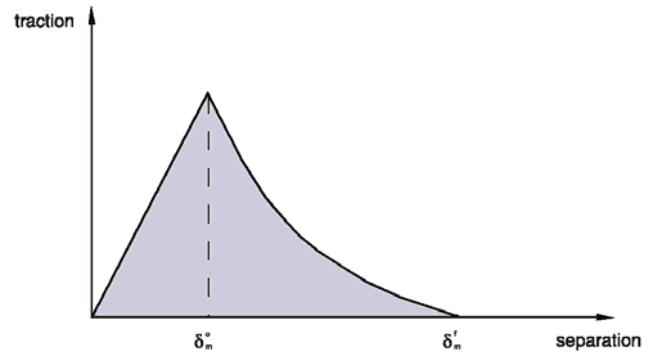


Figure 2. Traction-separation behaviour of cohesive elements.

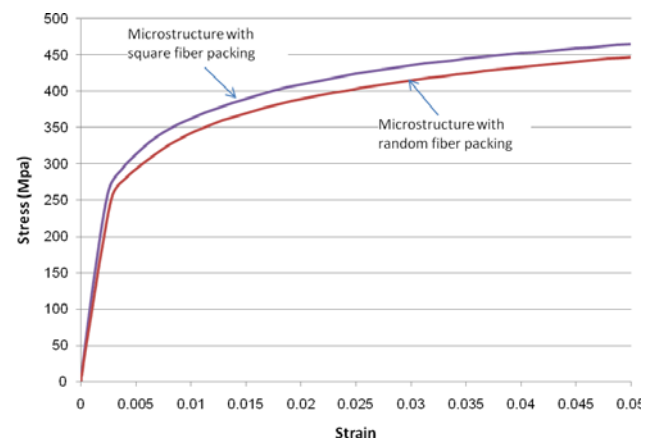


Figure 3. Cauchy stress required to applied elastic-plastic tensile transverse deformation to graphite/aluminum composite with different microstructures.

### B. Transverse Loading with Damage Evolution

The damage initiation is defined based on the normal and shear strengths of the cohesive elements considered at the fiber–matrix interface in graphite/aluminum metal matrix composite. The shear strength is related to the normal strength as  $t_s^0 = t_t^0 = t_n^0 / \sqrt{3}$  and the normal strength is varied to evaluate the effects of bonding strength on stress-strain graph of composite material. The fiber-matrix debonding is assumed to be occurred when the effective displacement reaches to 100  $\mu\text{m}$ . The interfacial fracture energy in Mode I and II can be calculated based on the area under the traction-separation curve. Fig. 4 illustrates the deformed geometry of RUC considered for microstructures with square and random fiber packing patterns, in which the normal strength of cohesive zone is 200 MPa. The deformation of RUC corresponds to the local macroscopic transverse strain of 0.02 which leads to the debonding in the fiber-matrix interface considering normal strength of  $t_n=100$  MPa. In the microstructure with regular square packing, the applied tensile strain causes that lateral compressive stress is observed in the cohesive zones at the plane normal to the loading direction. Since the cohesive failure is insensitive to compressive stress, no separation is observed at this region, as shown in Fig. 4a. On the other hand, the interface starts to separate at the plane parallel to the loading direction located on the lines at the top and bottom surfaces of fiber because of cohesive failure at the tensile loading. After the separation at top and bottom surface of fiber, combined tensile and shear loadings are applied to the cohesive elements causing to propagate the separation toward the plane normal to the transverse loading. In the microstructure with random fiber packing, there is no symmetry for loading condition of fibers and the fiber-matrix separation may be observed at different points, as observed in Fig. 4b.

The stress-strain curves of the graphite/aluminum metal matrix composite are shown in Fig. 5 considering the damage evolution in the fiber-matrix interface. The graphs start with a linear elastic region with the same transverse elastic modulus. Based on the normal strength of cohesive elements, nonlinear plastic deformation is observed at different stress levels. As shown in Fig. 5a, the stress-strain graphs of RUC with regular fiber packing have abrupt stress falls as the debonding occurs, because the applied stress to the fiber drops and the matrix should carry the transverse loading. Since the matrix is the only material subjected to the transverse loading when the complete debonding occurs in the fiber-matrix interface, the stress level decreases to the same level in different values for cohesive strength. The transition between ideal stress-strain graph to stress level in the matrix material is observed in more strain for cohesive material with higher strength. The multiple stress drops are observed for the microstructure with random fiber packing, as shown in Fig. 5b. Each stress drop corresponds to the initiation of matrix separation from the fibers distributed in the microstructure. Since progressive damage correlates with

the experimental observation, the micromechanical modeling yields accurate results for microstructure with random fiber packing

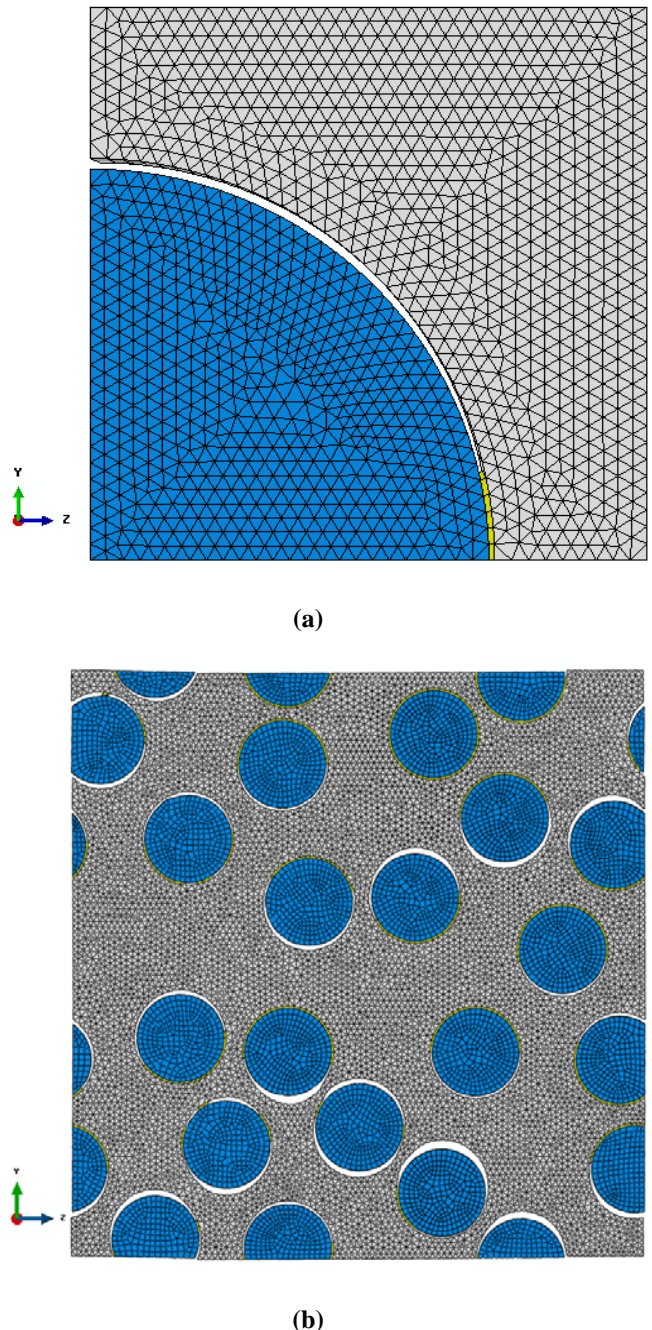


Figure 4. Deformed geometries of matrix, fiber and cohesive elements subjected to tensile axial deformation normal to fiber direction in the RUC of graphite/aluminum composite having 0.4 fiber volume fraction and  $t_n=100$  MPa and microstructures with a) square fiber packing b) random fiber packing.

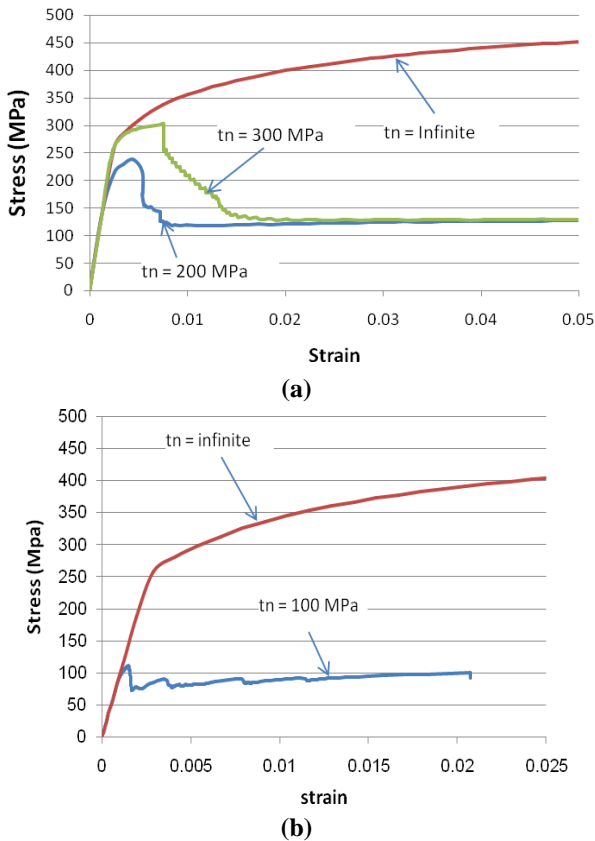


Figure 5. Cauchy stress required to applied elastic-plastic tensile transverse deformation to graphite/aluminum composite in different strength of fiber-matrix interface for microstructures with a) square fiber packing b) random fiber packing.

VI. CONCLUSIONS

The local fiber distribution significantly affects the interfacial stress state and the onset and evolution of fiber-matrix debonding. As the local damage is initiated at the fiber-matrix interface of the microstructure with ideal square fiber packing, it propagates to the total interfacial zone for a negligible strain increase. In the microstructures with ideal square fiber packing, the stress drop is observed in the stress-strain curve due to stress releasing in the fiber materials. As the complete debonding occurs in the fiber-matrix interface, the matrix is the only material subjected to the transverse loading. Therefore, the stress level decreases to the same level for microstructures having cohesive elements with different strength values. Progressive damage evolution is observed in the fiber-matrix interfaces of the microstructure with random fiber packing, in which each stress drop corresponds to the initiation of matrix separation from the fibers distributed in the microstructure. The transition between ideal stress-strain curves to stress levels in the matrix material is observed in more strain for cohesive material with higher strength. The damage evolution starts at lower stress level in the microstructure with random fiber packing compared

to the regular microstructure and the transverse stress converges to the same level in both microstructures at high strain value.

REFERENCES

- [1] S. Ghosh, Y. Ling, B. Majumdar, and R. Kim, "Interfacial debonding analysis in multiple fiber reinforced composites", *Mechanics of Materials*, vol. 32, pp. 561-591, October 2000
- [2] T. Hobbiebrunken, M. Hojo, T. Adachi, C. De Jong, and B. Fiedler, "Evaluation of interfacial strength in CF/epoxies using FEM and in-situ experiments", *Composite Part A – Applied Science*, vol. 37(12), pp. 2248–56, December 2006.
- [3] EK. Gamstedt and BA. Sjögren, "Micromechanisms in tension-compression fatigue of composite laminates containing transverse plies", *Composite Science Technology*, vol. 59(2), pp. 167–78, February 1999.
- [4] T.J. Vaughan and C.T. McCarthy, "Micromechanical modelling of the transverse damage behavior in fiber reinforced composites", *Composite Science Technology*, vol. 71, pp. 388–396, February 2011.
- [5] E. Totry, C. González, and J. Llorca. "Failure locus of fiber-reinforced composites under transverse compression and out-of-plane shear", *Composite Science Technology*, vol.68(3–4), pp. 829-39, March 2008.
- [6] N. Chandra, H. Li, C. Shet, and H. Ghonem, "Some issues in the application of cohesive zone models for metal-ceramic interfaces", *Int J Solids Structure*, vol. 39, pp. 2827–2855, May 2002.
- [7] N. Chandra and H. Ghonem, "Interfacial mechanics of push-out tests: theory and experiments". *Composite Part A – Applied Science*, vol. 32 (3–4), pp. 575–584, March–April 2001.
- [8] M-J. Pindera, H. Khatam, A.S. Drago, and Y. Bansal, "Micromechanics of spatially uniform heterogeneous media: A critical review and emerging approaches", *Composite Part B*, vol. 40, pp. 349–378, July 2009.
- [9] M.T. Abadi, "Micromechanical modeling of heterogeneous materials at finite strain," in *Wiley Encyclopedia of composite*, Nicolais, A. Borzacchiello, Wiley, 2012, pp. 1778–1791.
- [10] R. von Mises, "Mechanik der festen Körper im plastisch deformablen Zustand. Götting", *Nachr. Math. Phys.*, vol. 1, pp. 582–592, 1913.
- [11] W. Ramberg and W. R. Osgood, "Description of stress-strain curves by three parameters". Technical Note No. 902, National Advisory Committee For Aeronautics, Washington DC, 1943.
- [12] A. A. Gusev, P. J. Hine, and I. M. Ward, "Fiber packing and elastic properties of a transversely random unidirectional glass/epoxy composite", *Composite Science Technology*, Vol. 60 (4), pp. 535-541, March 2000.
- [13] R.J.M. Smit, W.A.M. Brekelmans, and H.E.H.Meijer, "Prediction of the mechanical behavior of nonlinear heterogeneous system by multi-level finite element modeling", *Computer Methods Applied Mechanics. Eng.* vol. 155, pp. 181-192, March 1998.
- [14] J.S. Wang, "Random sequential adsorption, series expansion and Monte Carlo simulation", *Physics A*, vol. 254, pp. 179–184, May 1998.
- [15] P.P. Camanho and C.G. Davila, Mixed-mode decohesion finite elements for the simulation of delamination in composite materials, NASA/TM-2002-211737, Langley Research Center, Hampton, Virginia, June 2002.